UDC 621.314 https://doi.org/10.20998/2074-272X.2025.3.09

B. Dwinanto, Setiyono, F. Thalib, H. Siswono

Single-phase power shunt active filter design using photovoltaic as reactive power compensator

Introduction. *The rapid production of electronic equipment circulating and used by the public has resulted in a decline in the power quality in the power system.* ***The goal*** *of the article is to build a parallel active filter for reactive power compensation in a single-phase power system using photovoltaic (PV) as the input DC link voltage for the inverter through simulation modeling using MATLAB/Simulink.* ***Methods.*** *The method used is to design a parallel active filter modeling for a single-phase electrical network that serves loads in the form of AC DC converters with inductive recessive and capacitive recessive loads using MATLAB/Simulink.* ***Results.*** *The simulation results show that the total harmonic distortion (THD) value of the system before being screened is 37.93 % for inductive resistive loads and 18.77 % for capacitive resistive loads, and after going through screening the THD value can drop significantly by 0.35 % for inductive resistive loads and 1.45 % for resistive capacitive loads.* ***Practical value.*** *PV systems can be used as power generators to provide a voltage of 800 V on a single-phase parallel active power filter using a voltage source inverter.* References 30, table 2, figures 11.
Key words: **active shunt filter, compensator, photovoltaic, reactive power, voltage source inverter.**

Вступ. *Швидке виробництво електронного обладнання, яке використовується населенням, призвело до зниження якості електроенергії в енергосистемі.* ***Метою*** *статті є побудова паралельного активного фільтра для компенсації реактивної потужності в однофазній енергосистемі з використанням фотоелектричних (PV) елементів як вхідної напруги постійного струму для інвертора за допомогою імітаційного моделювання з використанням MATLAB/Simulink.* ***Методи***. *Використовуваний метод полягає у розробці моделювання паралельного активного фільтра для однофазної електричної мережі, яка обслуговує навантаження у вигляді перетворювачів змінного струму у постійний з індуктивними рецесивними і ремісивними ємнісними навантаженнями з використанням MATLAB/Simulink.* ***Результати*** *моделювання показують, що значення повного гармонійного спотворення (THD) системи перед екрануванням становить 37,93 % для індуктивних резистивних навантажень і 18,77 % для ємнісних резистивних навантажень, а після проходження екранування значення THD може значно знизитися на 0,35 % для індуктивних резистивних навантажень і 1,45 % для резистивних ємнісних навантажень.* ***Практична цінність***. *PV системи можуть використовуватися як генератори енергії для забезпечення напруги 800 В на однофазному паралельному активному фільтрі потужності з використанням інвертора напруги.* Бібл. 30, табл. 2, рис. 11.
Ключові слова: **активний шунтуючий фільтр, компенсатор, фотовольтаїка, реактивна потужність, інвертор напруги.**

Introduction. The rapid production of electronic equipment circulating and used by the public, such as computer equipment, power converters, and variable frequency drive systems for electric motors or devices based on power electronics, has resulted in a decline in the quality of power in the power system. Because of its nature, this load falls under the category of nonlinear loads. In power systems, the current has high wave distortion, leading to a large total harmonic distortion (THD). Excess heat generated by harmonics can cause power losses and reduce the efficiency of power equipment [1–3].

Various methods for reducing the presence of these harmonics include the use of filters. According to the configuration, there are 3 types of filters: passive, active, and hybrid (a combination of passive and active filters) [4, 5]. The harmonics of this power system occur in odd orders such as 150 Hz, 250 Hz and 350 Hz. Passive filters can be in the form of capacitive receptive (RC) or inductive receptive (RL) elements and are generally used to reduce the highest harmonic distortion at selected frequencies or tune at frequencies that are more dominantly disturbing, and the THD value can be reduced significantly [6, 7].

An active filter is a series of filters that use passive and active electronic elements originating from electronic devices such as operational amplifiers, MOSFETs and transistors in the form of inverters that produce reverse current or anti-harmonics [4]. The output of the inverter is controlled through ignition pulses, one of which uses hysterical current control [8]. Shunt active power filters (SAPFs) offer greater benefits than typical filter solutions because of their ability to map the injection currents more accurately, resulting in economic advantages [9, 10]. Hybrid filters, on the other hand, are a combination of passive and active filters that are commonly utilized in aluminum smelting plants to manage harmonic attenuation [11]. This filter is classified into 2 types, series active filters and parallel active filters, based on their configuration. Series active filters were used to eliminate current harmonics, whereas parallel active filters were used to reduce voltage harmonics.

The efficiency of active filters is determined by various factors such as the control system, filter reactor, DC link capacitor parameters, and electrical system. To achieve improved power quality, three components are necessary: power compensation for current and voltage waveform distortions, reactive power compensation, and compensation for load imbalance [12]. Solar energy is increasingly being used to compensate for the reactive power in electric power systems. In particular, the use of renewable energy, such as solar energy, has been developed for various applications. One such application is the use of SAPF technology. Compared to a thyristor bridge on a voltage source inverter (VSI) with an input reactor inductance equal to or smaller than the input reactor inductance of the SAPF, the SAPF is more efficient in terms of reactive power and harmonic attenuation [13].

Photovoltaic (PV) is practically an endless energy resource, which has made it highly essential recently, especially for electrical power applications in high-luminosity countries [14]. PV technology is a renewable way of converting solar energy into electrical energy. It can be used to address the current harmonics in power systems with parallel active filters [15, 16]. There are 2 varieties of PV systems: grid-connected and stand-alone. Because of its easy energy conversion process and modular scaling, grid-connected PV systems have been used extensively in the commercial sector [17]. When a stand-alone PV system is connected to the grid, it produces fluctuations in the output voltage owing to changes in temperature and irradiation. This makes it necessary to control the voltage and power quality, particularly when unbalanced load conditions occur. This control helps minimize the ripples on the DC

link [18, 19]. The use of PV solar energy is essential to the shift to a low-carbon economy [20].

The goal of the paper is to build a parallel active filter for reactive power compensation in a single-phase power system using PV as the input DC link voltage for the inverter through simulation modeling using the MATLAB/Simulink.

Subject of investigations. This study involved the development of a simulation of the compensation current I_C injected into a single-phase power system with a linear load. Basic concept of parallel SAPF is shown in Fig. 1.

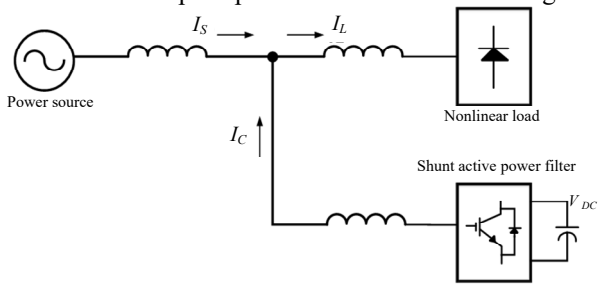

Fig. 1. Basic concept of parallel SAPF

The compensation of the harmonic currents is performed using a closed-loop controlled active power filter. This filter injects a compensation current I_C into the power system mesh whenever the load changes. Based on Fig. 1, the source current I_S can be represented as:

$$i_S = i_L - i_C, \quad (1)$$

where i_S is the source current; i_L is the load current; i_C is the compensation current.

The modeling design of the parallel active filter circuit is shown in Fig. 2.

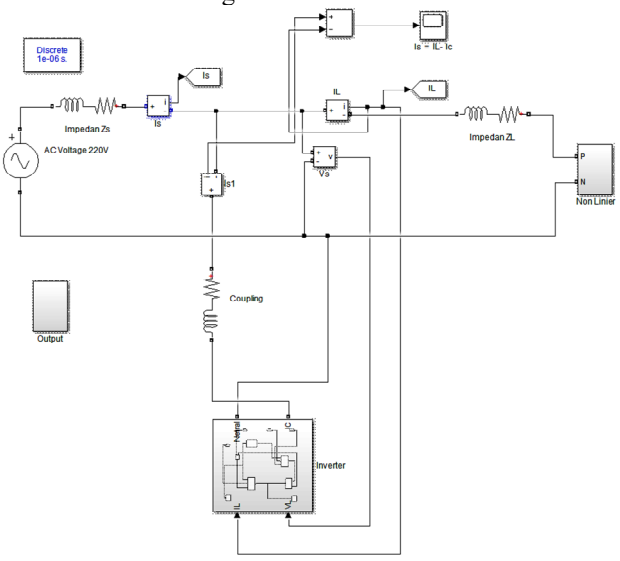

Fig. 2. Single-phase parallel active filter design using PV as a compensator

This circuit involves a single-phase voltage source connected to a nonlinear load, and is equipped with a parallel active filter. The filter comprises a series of low-pass filters and multiple active semiconductor components that collaborate to regulate the shape of the harmonic interference at every frequency order. The compensation current is generated by causing anti-harmonics in the current, which are affected by harmonics. Subsequently, this compensation current is introduced into the circuit. Schematic block of the overall model circuit shown in Fig. 3.

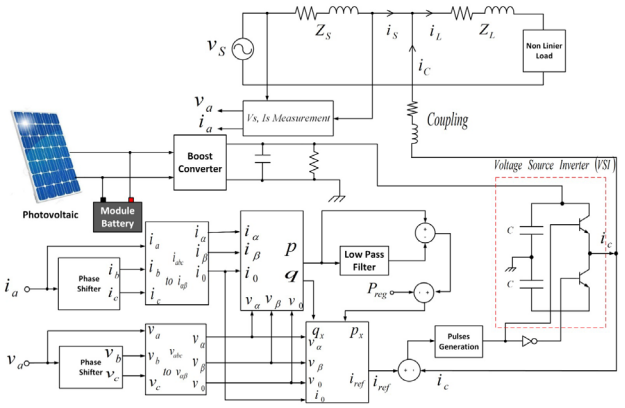

Fig. 3. Schematic block of the overall model circuit

The system has a complete design that includes 3 main parts: a DC power source PV system, a SAPF and a single-phase power system with a nonlinear load. The PV system is a DC power generator that produces 29.3 V voltage and a maximum short circuit current of 7.97 A. To meet the voltage requirements of the VSI, the voltage is increased through a booster circuit to 800 V [21–24]. The filtering process in an electrical system requires a battery module to store energy. The power filter, also known as an active shunt filter, generates a reference current i_{ref}. This process involved multiple stages. In the first stage, a voltage sensor and current sensor measured the magnitudes of the source current and source voltage, respectively. In this study, a single-phase voltage system was used. However, the power quality (PQ) theory is more suitable for 3-phase systems. Therefore, a virtual voltage and current source were created to obtain the parameters v_a, v_b, v_c, i_a, i_b, and i_c. After obtaining these parameters, the next step is to transform them into α–β coordinates. This transformation is known as Clark transformation and is essential for obtaining the i_{ref} quantity.

Results. Static calculations. This section discusses the results presented in the form of pictures, graphs, tables, etc. to make it easier for readers to understand them.

Clark transformation. Mathematical transformation calculations were performed to obtain the single-phase reference current. The reference current generation flow was based on the PQ theory discovered by Akagi in 1983. This theory was presented in [25]. PQ theory is best suited for 3-phase systems. To apply it to single-phase systems or to obtain the other 2-phases, virtual voltages and currents must be created for phases B and C that are 120° apart from phase A. The virtual voltages and currents for phases B and C can be derived from the voltage and current of phase A by shifting them 120° and –120°, respectively:

$$\begin{aligned} v_A &= V_m \sin(\omega t); \\ v_B &= V_m \sin(\omega t + 120°); \\ v_C &= V_m \sin(\omega t - 120°), \end{aligned} \quad (2)$$

where v_A, v_B, v_C are the voltages of phases A, B, C.

Reference signal generation algorithm. Once the virtual voltage and current parameters were obtained from the measurement results of a single-phase power system, the parameter values were converted into single-phase voltage system coordinates. This conversion involves transforming the absolute coordinates of the voltage and current to α–β coordinates using the PQ theory. This transformation is also known as Clark transformation [26, 27]. Reference current generation algorithm is shown in Fig. 4.

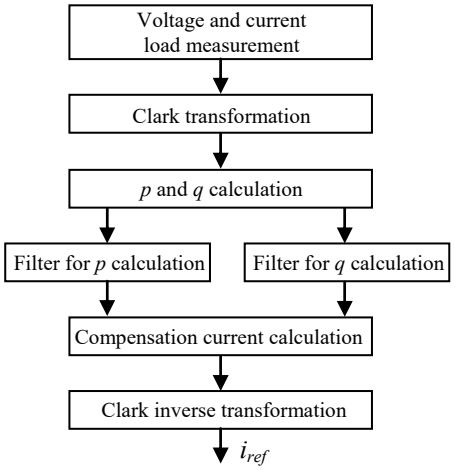

Fig. 4. Reference current generation algorithm

Shown in Fig. 4 is the flow for getting the voltage and current parameters v_α, v_β, i_α, i_β, v_0, i_0:

$$\begin{bmatrix} v_\alpha \\ v_\beta \end{bmatrix} = \sqrt{\frac{2}{3}} \begin{bmatrix} 1 & -1/2 & -1/2 \\ 0 & \sqrt{3}/2 & -\sqrt{3}/2 \end{bmatrix} \begin{bmatrix} v_A \\ v_B \\ v_C \end{bmatrix}; \quad (3)$$

$$\begin{bmatrix} i_\alpha \\ i_\beta \end{bmatrix} = \sqrt{\frac{2}{3}} \begin{bmatrix} 1 & -1/2 & -1/2 \\ 0 & \sqrt{3}/2 & -\sqrt{3}/2 \end{bmatrix} \begin{bmatrix} i_A \\ i_B \\ i_C \end{bmatrix}. \quad (4)$$

The voltages and currents in reference frames α and β are:

$$v_\alpha = \sqrt{\frac{2}{3}} v_A - \frac{1}{\sqrt{6}} v_B - \frac{1}{\sqrt{6}} v_C; \quad (5)$$

$$v_\beta = \frac{1}{\sqrt{6}} v_B - \frac{1}{\sqrt{6}} v_C; \quad (6)$$

$$i_\alpha = \sqrt{\frac{2}{3}} i_A - \frac{1}{\sqrt{6}} i_B - \frac{1}{\sqrt{6}} i_C; \quad (7)$$

$$i_\beta = \frac{1}{\sqrt{6}} i_B - \frac{1}{\sqrt{6}} i_C. \quad (8)$$

The next step is to determine or calculate the values of the active p and the reactive q powers:

$$\begin{bmatrix} p \\ q \end{bmatrix} = \begin{bmatrix} v_\alpha & v_\beta \\ -v_\beta & -v_\alpha \end{bmatrix} \begin{bmatrix} i_\alpha \\ i_\beta \end{bmatrix}. \quad (9)$$

Equation (9) shows that the instantaneous active power p is equal to the sum of $p = v_\alpha i_\alpha + v_\beta i_\beta = \overline{p} + \widetilde{p}$, which can be broken down into 2 components: the $\overline{p}$ component (DC component value) and the $\widetilde{p}$ component (AC component value). The $\overline{p}$ component is the instantaneous average power transferred from the source to the load, whereas the $\widetilde{p}$ component is the average power exchanged between the source and load via ABC coordinates. However, the $\widetilde{p}$ component does not transfer energy from the source to the load; therefore, it must be removed with a filter:

$$\begin{bmatrix} i_{c\alpha} \\ i_{c\beta} \end{bmatrix} = \frac{1}{v_\alpha^2 + v_\beta^2} \begin{bmatrix} v_\alpha & -v_\beta \\ v_\beta & v_\alpha \end{bmatrix} \begin{bmatrix} \widetilde{p} - \Delta\overline{p} \\ q \end{bmatrix}, \quad (10)$$

where $i_{c\alpha}$, $i_{c\beta}$ are the compensation currents in reference frames α and β; $\widetilde{p}$ is the alternating active power component; $\Delta\overline{p}$ is the total direct active power component; q is the reactive power component.

After obtaining the p components, a reverse transformation is carried out to obtain the reference current value [28]:

$$\begin{bmatrix} i_{c\alpha} \\ i_{c\beta} \end{bmatrix} = \frac{1}{v_\alpha^2 + v_\beta^2} \begin{bmatrix} v_\alpha & -v_\beta \\ v_\beta & v_\alpha \end{bmatrix} \begin{bmatrix} p_x \\ q_x \end{bmatrix}, \quad (11)$$

$p_x = \widetilde{p} - \Delta\overline{p}$ and $\Delta\overline{p} = \overline{p}_0$ then $q_x = q = \overline{q} + \widetilde{q}$, where p_x is the unwanted active power component; q_x is the unwanted reactive power component; $\overline{p}_0$ is the active power zero sequence component; $\overline{q}$ is the direct reactive power component; $\widetilde{q}$ is the alternating reactive power component.

The single-phase reference current can be defined as:

$$i_{ref} = \sqrt{\frac{2}{3}} \left[\frac{p_x v_\alpha - q_x v_\beta}{v_\alpha^2 + v_\beta^2} + \frac{i_0}{\sqrt{2}} \right]; \quad (12)$$

where i_0 is the zero sequence current.

Parameter values of the modeling system are presented in Table 1.

Table 1

Parameter values of the modeling system

Parameter	Value	Parameter	Value
Single-phase AC input voltage	220 V	Frequency	50 Hz
Input impedance	R=0.5 Ω; L=35 mH	Load impedance	R_L=20 Ω, L_L=5 mH
Coupling impedance (smoothing)	R_c=1 Ω; L_c=3.5 mH	DC link capacitor	C_1=C_2= 400 V, 50 nF
AC-DC converter	Bridge rectifier diode	Rectifier load	*RL* (R=50 Ω, L= 15 mH; *RC* (R=50 Ω, C = 1,5 nF
K_p	3	K_i	1
PV max power	218.87 W	Open circuit voltage	36.6 V
Max power point voltage	29.3 V	Current short circuit	7.97 A

A boost converter regulator was used to increase the DC input voltage from the battery without the need for a transformer. Figure 5 shows the operation of the boost converter circuit, which can be divided into 2 modes. Mode 1 begins when switch S is turned ON at t = 0. The input current increases, the inductor is formed by a magnetic field with a voltage of $V_L = L\frac{\mathrm{d}i_L}{\mathrm{d}t}$; $C\frac{\mathrm{d}V_C}{\mathrm{d}t} + \frac{V_C}{R} = 0$ and the current increases with a constant slope. This state is $V_{DC} = V_L$. Mode 2 begins when switch S is turned OFF at t = 1. The current flows through L, the diode D and C. The inductor current decreases until switch S is turned on again during the next cycle.

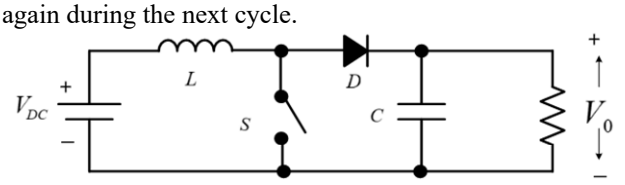

Fig. 5. Boost converter circuit

When switch S is in the OFF mode, $V_{DC} = V_L + V_C$, the voltage across the circuit is the sum of the voltages across the inductor and capacitor. This implies that $L\frac{\mathrm{d}i_L}{\mathrm{d}t} = V_{DC} - V_C$,

where $\frac{di_L}{dt} = \frac{V_{DC} - V_C}{L}$. In this situation, the current decreases, eventually reaching the same level as that when the switch is ON. During the gate switch switching on current, the output current wave pattern increases by $I_{max} - I_{min} = V_{DC} \cdot k / L$, where k is the duty cycle. Similarly, when the switch is turned OFF, the current decreases to $I_{min} - I_{max} = \frac{V_{DC} - V_C}{L}(1-k)$, where

$$V_0 = V_C = \frac{V_{DC}}{1-k}. \quad (13)$$

To increase the input voltage, multiple stages of the boost converter can be arranged, resulting in a conversion ratio that is always higher than that of a single boost converter. This type of converter can be used in various applications, such as Microgrid systems, electric trains, UPS, inverters and wireless energy transfer [24].

PI controller. When an active filter injects a current into the power system, it must always be greater than the current flowing from the source to the load. To achieve this, the voltage of the VSI must be greater than the wire-to-wire voltage of the single-phase source and must be kept constant. PI controller was used to regulate the DC voltage by adjusting the K_p and K_i values [29]. PI controller block is shown in Fig. 6.

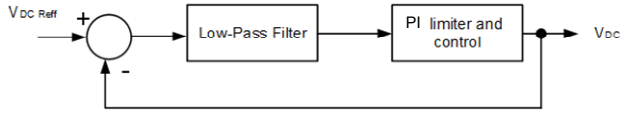

Fig. 6. PI controller block

Voltage source inverter (VSI) is a powerful power conditioner used in active filters. One of the reasons to consider using a VSI over the current source inverter is that it is easier to control the current compared to current source inverter. A VSI uses capacitors for DC energy storage. The single-phase VSI circuit comprises 2 electronic switches that can be in the form of a MOSFET or power transistor placed in parallel with a capacitor bank. MOSFETs are generally preferred for fast switching and low-frequency applications [30]. Table 2 provides information on the relationship between the switch conditions and VSI output voltage. Figure 7 shows the single-phase inverter.

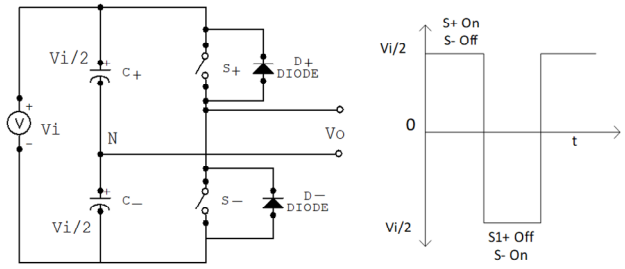

Fig. 7. Single-phase inverter

Table 2

Operation of switches on the inverter

No.	Condition	v_0	Active components
1	S+ ON and S– OFF	$v_i/2$	S+ if $i_0>0$; D+ if $i_0<0$
2	S+ OFF and S– ON	$-v_i/2$	D– if $i_0>0$; S– if $i_0<0$
3	S+ and S– OFF	$-v_i/2$ and $v_i/2$	D– if $i_0>0$; D+ if $i_0<0$

The S+ and S– switches must not operate at the same time, as this can cause a short circuit. The ON and OFF states of the S+ and S– switches are controlled using a modulation technique, specifically pulse width modulation (PWM). The PWM principle in this circuit compares the modulation signal V_C (in this case the expected output alternating voltage) with a carrier signal with a saw waveform (V_Δ). Practically, if $V_C > V_\Delta$ then the S+ switch will be ON and the S– switch will be OFF, and if $V_C < V_\Delta$, then the S+ switch will be OFF and the S– switch will be ON.

RC load observation. Observations and tests were conducted on nonlinear, *RC* and *RL* loads to observe the sinusoidal current waveform patterns before and after filtering. Display of load current, compensation current and source current with non-linear and *RC* loads is shown in Fig. 8, which shows the distorted capacitive load current waveform. The waveform was no longer a pure sinusoidal pattern and appeared uneven. The middle image represents the compensation current waveform injected into the power line. Finally, the last image displays the current waveform that has been compensated for by the injected current, and its shape now returns to a sinusoidal pattern.

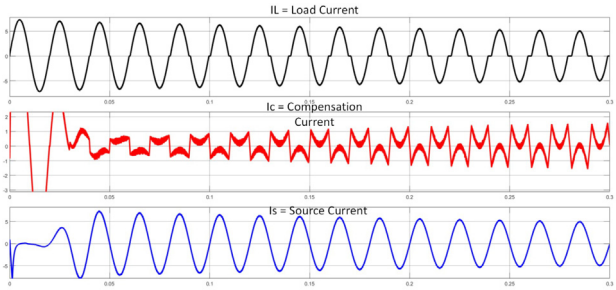

Fig. 8. Display of load current, compensation current and source current with non-linear and *RC* loads

THD measurement for *RC* loads using fast Fourier transform (FFT) is shown in Fig. 9.

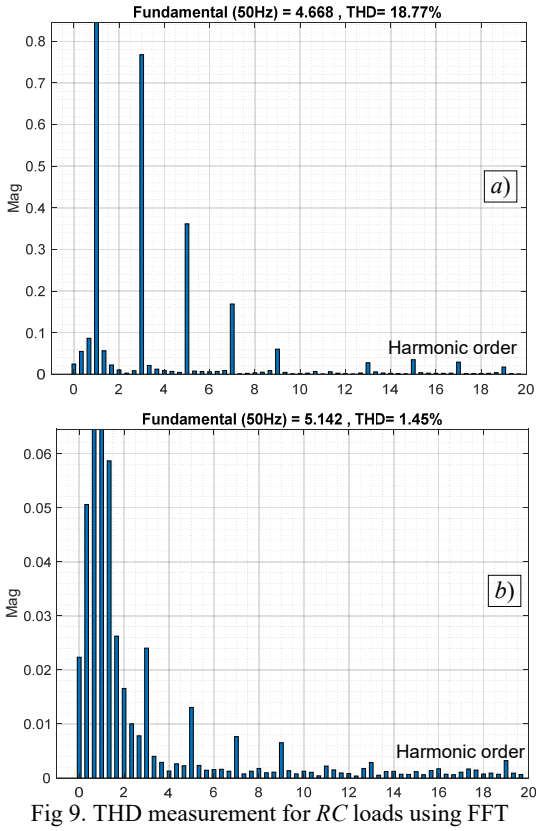

Fig 9. THD measurement for *RC* loads using FFT

Figure 9,*a* shows odd-order harmonic interference at 250, 350, 550, 850 and 950 Hz. Index THD before compensation indicating a value of 18,77 %. The 5th order harmonic was the largest at 250 Hz. Figure 9,*b* shows that the compensation current reduces the THD to 1.45 %.

***RL* load observation.** Display of load current, compensation current and source current with non-linear and *RL* loads is shown in Fig. 10, which shows 3 different current waveforms. The first image depicts a distorted waveform that appears almost square, caused by nonlinear and *RL* loads. The middle image shows the compensation current waveform, whereas the bottom image shows the source-current waveform after the compensation current is applied.

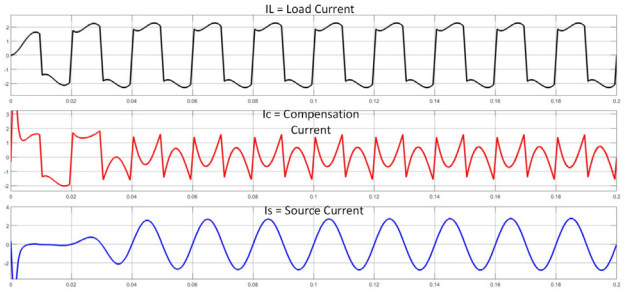

Fig. 10. Display of load current, compensation current and source current with non-linear and *RL* loads

Figure 11 shows the THD measurement at *RL* load using FFT. Figure 11,*a* shows a graph of the THD index before compensation, indicating a value of 36.93 %. Meanwhile, Figure 11,*b* displays a THD index of 0.48 % after filtering.

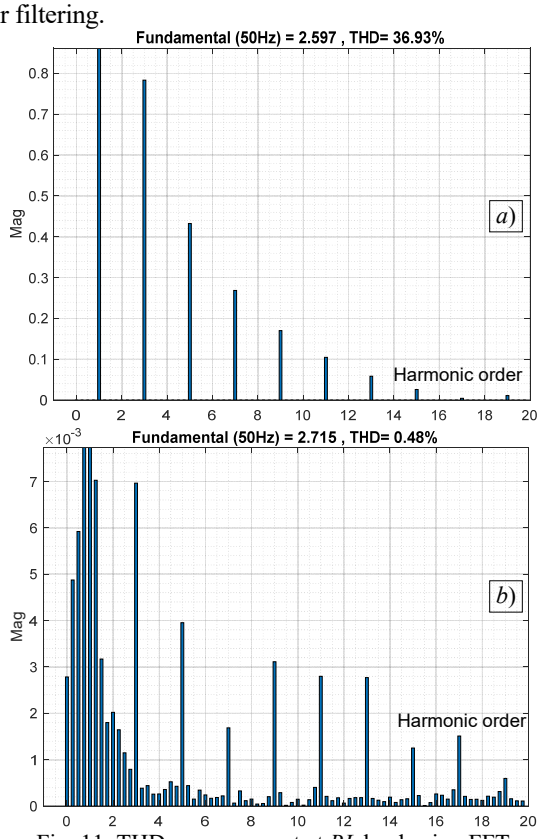

Fig. 11. THD measurement at *RL* load using FFT

Conclusions. The PV systems can be used as a power generator to provide a voltage of 800 V on a single-phase parallel active power filter using a voltage source inverter. This voltage value is achieved by increasing the DC voltage from the boost converter circuit. The PV power can also be used as a reactive power compensator to prevent the presence of harmonics in single-phase power systems. The DC link capacitor functions as a compensation current pattern generator. The instantaneous power theory, which is commonly used in 3-phase power systems, can also be applied to single-phase systems by adding two virtual voltage sources that resemble a 3-phase voltage source. The compensation current has a waveform that is similar to the reference current, and it is obtained through mathematical calculations of the Clark transformation. Test results have shown that this parallel active filter can reduce the THD from 18.77 % to 1.45 % on capacitive loads, and it can reduce the THD value from 37.97 % to 0.48 % on inductive loads.

Acknowledgements. We would like to thank Gunadarma University as the author's institution for its support and assistance during the research. Similarly, thanks to the advice and input from Prof. Ir. Bosono Soerowirjo, PhD, as supervisor for this research.

Conflicts of interest. The authors declare no conflict of interest.

REFERENCES

1. Badoni M., Singh A., Singh B. Adaptive recursive inverse-based control algorithm for shunt active power filter. *IET Power Electronics*, 2016, vol. 9, no. 5, pp. 1053-1064. doi: https://doi.org/10.1049/iet-pel.2015.0170.

2. Sozański K. Three phase active power filter with selective harmonics elimination. *Archives of Electrical Engineering*, 2016, vol. 65, no. 1, pp. 33-44. doi: https://doi.org/10.1515/aee-2016-0003.

3. Alhmoud L. THD Reduction Using Shunt Active Power Filter: A Real Case Study. *Universal Journal of Electrical and Electronic Engineering*, 2019, vol. 6, no. 4, pp. 259-264. doi: https://doi.org/10.13189/ujeee.2019.060407.

4. Alhamrouni I., Hanafi F.N., Salem M., Rahman N.H.A., Jusoh A., Sutikno T. Design of shunt hybrid active power filter for compensating harmonic currents and reactive power. *TELKOMNIKA (Telecommunication Computing Electronics and Control)*, 2020, vol. 18, no. 4, pp. 2148-2157. doi: https://doi.org/10.12928/telkomnika.v18i4.15156.

5. Albasri F.A., Al-Mawsawi S.A., Al-Mahari M. A pot line rectiformer scheme with hybrid-shunt active power filter. *International Journal of Power Electronics and Drive Systems (IJPEDS)*, 2022, vol. 13, no. 1, pp. 1-10. doi: https://doi.org/10.11591/ijpeds.v13.i1.pp1-10.

6. Madhu B.R., Dinesh M.N., Ravitheja B.M. Design of shunt hybrid active power filter (SHAPF) to reduce harmonics in AC side due to Non-linear loads. *International Journal of Power Electronics and Drive Systems (IJPEDS)*, 2018, vol. 9, no. 4, pp. 1926-1936. doi: https://doi.org/10.11591/ijpeds.v9.i4.pp1926-1936.

7. Firoozian M., Hosseinian S.H., Abedi M. A new innovative current controller for selective harmonic compensation using active power filters in a microgrid with renewable energy source. *International Journal of Power Electronics and Drive Systems (IJPEDS)*, 2022, vol. 13, no. 4, pp. 2396-2404. doi: https://doi.org/10.11591/ijpeds.v13.i4.pp2396-2404.

8. Raja Mohamed S., Jeyanthy P.A., Devaraj D. Hysteresis-based Voltage and Current Control Techniques for Grid Connected Solar Photovoltaic Systems: Comparative Study. *International Journal of Electrical and Computer Engineering (IJECE)*, 2018, vol. 8, no. 5, pp. 2671-2681. doi: https://doi.org/10.11591/ijece.v8i5.pp2671-2681.

9. Barnabé F., Rocha M., Clerice G. Enhancement of Power Quality Using Voltage and Hall Effect Current Sensors Applied on Controlled Single-Phase Active Power Filter. *Engineering Proceedings*, 2020, vol. 2, no. 1, art. no. 74. doi: https://doi.org/10.3390/ecsa-7-08212.

10. Gwóźdź M., Ciepliński Ł. An active power filter based on a hybrid converter topology – Part 1. *Bulletin of the Polish Academy of Sciences Technical Sciences*, 2021, vol. 69, no. 1, art. no. e136218. doi: https://doi.org/10.24425/bpasts.2020.136218.

11. Akagi H. Modern active filters and traditional passive filters. *Bulletin of the Polish Academy of Sciences: Technical Sciences*, 2006, vol. 54, no. 3, pp. 255-269.

12. Szromba A. Improving the Efficiency of the Shunt Active Power Filter Acting with the Use of the Hysteresis Current Control Technique. *Energies*, 2023, vol. 16, no. 10, art. no. 4080. doi: https://doi.org/10.3390/en16104080.
13. Azebaze Mboving C.S., Hanzelka Z. Analysis of the Influence of the 6-Pulse Thyristor-Bridge Input Reactor Size on the Shunt Active Power Filter Work Efficiency: A Case Study. *Energies*, 2023, vol. 17, no. 1, art. no. 80. doi: https://doi.org/10.3390/en17010080.
14. Bounechba H., Boussaid A., Bouzid A. Experimental validation of fuzzy logic controller based on voltage perturbation algorithm in battery storage photovoltaic system. *Electrical Engineering & Electromechanics*, 2024, no. 5, pp. 20-27. doi: https://doi.org/10.20998/2074-272X.2024.5.03.
15. Rajakkannu R., Rangaswamy B. An Enhanced Modified Multiport Interleaved Flyback Converter for Photovoltaic-Shunt Active Power Filter (PV-SHAPF) Applications. *International Transactions on Electrical Energy Systems*, 2022, vol. 2022, art. no. 1537319. doi: https://doi.org/10.1155/2022/1537319.
16. Ertekin D., Baltaci K., Çelebi M. Advancing Renewable Energy: An Experimental Study of a Switched-Inductor, Switched-Capacitor Luo Boost Converter for Low-Voltage Applications. *Electronics*, 2023, vol. 12, no. 24, art. no. 5006. doi: https://doi.org/10.3390/electronics12245006.
17. Janardhan G., Surendra Babu N.N.V., Srinivas G.N. Single phase transformerless inverter for grid connected photovoltaic system with reduced leakage current. *Electrical Engineering & Electromechanics*, 2022, no. 5, pp. 36-40. doi: https://doi.org/10.20998/2074-272X.2022.5.06.
18. Mohammed F.A., Bahgat M.E., Elmasry S.S., Sharaf S.M. Design of a maximum power point tracking-based PID controller for DC converter of stand-alone PV system. *Journal of Electrical Systems and Information Technology*, 2022, vol. 9, no. 1, art. no. 9. doi: https://doi.org/10.1186/s43067-022-00050-5.
19. Alharbi M. Control Approach of Grid-Connected PV Inverter under Unbalanced Grid Conditions. *Processes*, 2024, vol. 12, no. 1, art. no. 212. doi: https://doi.org/10.3390/pr12010212.
20. Lanani A., Djamai D., Beddiaf A., Saidi A., Abboudi A. Photovoltaic system faults detection using fractional multiresolution signal decomposition. *Electrical Engineering & Electromechanics*, 2024, no. 4, pp. 48-54. doi: https://doi.org/10.20998/2074-272X.2024.4.06.
21. Shahir F.M., Aberoumandazar M., Babaei E. High Gain DC-DC Boost Converter Applied in Hybrid System of Photovoltaic and Battery. *2021 International Symposium on Devices, Circuits and Systems (ISDCS)*, 2021, pp. 1-4. doi: https://doi.org/10.1109/ISDCS52006.2021.9397922.
22. Palanisamy R., Vijayakumar K., Venkatachalam V., Narayanan R.M., Saravanakumar D., Saravanan K. Simulation of various DC-DC converters for photovoltaic system. *International Journal of Electrical and Computer Engineering (IJECE)*, 2019, vol. 9, no. 2, pp. 917-925. doi: https://doi.org/10.11591/ijece.v9i2.pp917-925.
23. Dos Santos P.M., Serralheiro A.J., Borges B., Torres J.P.N., Charas A. An Experimental Study on Step-Up DC–DC Converters for Organic Photovoltaic Cells. *Journal of Low Power Electronics and Applications*, 2022, vol. 12, no. 2, art. no. 20. doi: https://doi.org/10.3390/jlpea12020020.
24. Salau A.O., Eya C.U., Onyebuchi O.C. Nonzero Staircase Modulation Scheme for Switching DC-DC Boost Converter. *Journal of Control Science and Engineering*, 2020, vol. 2020, art. no. 8347462. doi: https://doi.org/10.1155/2020/8347462.
25. Watanabe E.H., Aredes M., Akagi H. The p-q theory for active filter control: some problems and solutions. *Sba: Controle & Automação Sociedade Brasileira de Automatica*, 2004, vol. 15, no. 1, pp. 78-84. doi: https://doi.org/10.1590/S0103-17592004000100010.
26. Babu M.B., Srinivas L.R., Karunakar T., Amarendra A., Reddy D.S., Ramu M., Swarup Kumar J.N.V.R., Tulasi Ram S.S. Power quality improvement based on VSHDE algorithm incorporating shunt active power filter. *Journal of Electrical Systems*, 2023, vol. 19, no. 1, pp. 1-12.
27. Khan A., Jaffery M.H., Javed Y., Arshad J., Rehman A.U., Khan R., Bajaj M., Kaabar M.K.A. Hardware-in-the-Loop Implementation and Performance Evaluation of Three-Phase Hybrid Shunt Active Power Filter for Power Quality Improvement. *Mathematical Problems in Engineering*, 2021, vol. 2021, art. no. 8032793. doi: https://doi.org/10.1155/2021/8032793.
28. Afonso J., Aredes M., Watanabe E., Martins J. Shunt active filter for power quality improvement. *International Conference UIE 2000 – "Electricity for a Sustainable Urban Development"*, Lisboa, Portugal, 1-4 Nov. 2000, pp. 683-691.
29. Abdolrasol M.G.M., Hannan M.A., Hussain S.M.S., Ustun T.S. Optimal PI controller based PSO optimization for PV inverter using SPWM techniques. *Energy Reports*, 2022, vol. 8, pp. 1003-1011. doi: https://doi.org/10.1016/j.egyr.2021.11.180.
30. Lahlaci M.E., Miloudi M., Miloudi H. Experimental electromagnetic compatibility of conducted electromagnetic interferences from an IGBT and a MOSFET in the power supply. *Electrical Engineering & Electromechanics*, 2024, no. 3, pp. 38-43. doi: https://doi.org/10.20998/2074-272X.2024.3.05.

Received 11.10.2024
Accepted 17.01.2025
Published 02.05.2025

B. Dwinanto[1], *Master of Electrical Engineering,*
Setiyono[1], *Doctor of Information Technology,*
F. Thalib[1], *Doctor of Electrical Engineering,*
H. Siswono[1], *Doctor of Electrical Engineering,*
[1] Department of Electrical Engineering,
Faculty of Industrial Technology,
Gunadarma University, Depok, Indonesia,
e-mail: bambang_dwi@staff.gunadarma.ac.id (Corresponding Author); setiyono@staff.gunadarma.ac.id; farid@staff.gunadarma.ac.id; hartono@staff.gunadarma.ac.id

How to cite this article:
Dwinanto B., Setiyono, Thalib F., Siswono H. Single-phase power shunt active filter design using photovoltaic as reactive power compensator. *Electrical Engineering & Electromechanics*, 2025, no. 3, pp. 59-64. doi: https://doi.org/10.20998/2074-272X.2025.3.09